Available online at www.sciencedirect.com
SCIENCE DIRECT®
PERGAMON
Journal of Asian Earth Sciences 23 (2004) 37–45
Journal of Asian Earth Sciences
www.elsevier.com/locate/jseaes

Mineralogy and geochemistry of the argentiferous Pb–Zn and Cu veins of the Çolaklí area, Elazig, Eastern Turkey

Ahmet Sagiroglu*, Ahmet Sasmaz

Department of Geology, Firat University, Elazig 23119, Turkey

Received 3 October 2002; revised 20 March 2003; accepted 20 March 2003

Abstract

The studied Pb–Zn and Cu veins occur as N–S trending and vertically dipping features in quartz diorite of Coniacian–Campanian Elazig Magmatic Complex. The complex has characteristics typical of arc magmatism and is composed of granitoids and, volcanic, subvolcanic and pyroclastic rocks.

The veins are 0.5–2.5 m. thick and their lengths reach up to 750 m. The ore of veins are either massive or disseminated in gangue of carbonate minerals, quartz and barite. The veins display two sets of mineral assemblages: (1) Pb–Zn veins are composed of galena, freibergite, barite, sphalerite, chalcopyrite, pyrite, a Pb–Cl phase and native silver; (2) Cu veins have a mineral association of chalcopyrite, pyrite, galena, sphalerite, cubanite, bismuthinite and fahlore. The ore bodies are accompanied by narrow but intensely developed wall rock alterations of argillization, carbonatization and silicification.

Chemical analyses of ore samples indicate high Pb, Ag, Sb, Zn, Ba and Cu contents in the veins and high correlation values between Pb–Ag, Pb–Ba, Pb–Zn, Sb–Ag, Cd–Sb and Ba–Cd.

The REE geochemistry points to ore deposition under acidic conditions and probably as a product of the final stages of magmatism. Field, microscopic and geochemical data also indicate that the ores are related to the last phases of the magmatic activity of the Elazig Magmatic Complex.

Keywords: Ag–Pb–Cu veins; Freibergite; Pb–Cl phase; Elazig Magmatic Complex; Eastern Turkey

1. Introduction

The studied veins are located in the vicinity of Çolaklí village in the Elazig province which itself is located in the Eastern Tauride Region and is well known for many valuable ore deposits. These include examples of Alpin type chromite deposits at Guleman, several Cyprus- type massive sulphide deposits along the Southeastern Thrust Zone and argentiferous Pb–Zn deposits at Keban (Fig. 1). Other mineral resources of the province and the ore formations associated with the Elazig Magmatic Complex, have been the subject of several studies in recent years: Cu ores in granitic rocks by Sagiroglu (1986) and Sagiroglu and Preston (1987), vein type Pb–Zn and Cu ores by Sasmaz and Sagiroglu (1990, 1999), pyrometasomatic Fe and Ti mineralizations by Sagiroglu (1992) and Akgül and Sasmaz (1996). The general geology of the area and petrography of Elazig Magmatic Complex are described by Yazgan (1984), Bingöl (1984), Asutay (1985) and Akgül (1993).

The Çolaklí ore veins are located north of Çolaklí village, 20 km north of Elazig town (Fig. 2) and occur in quartz diorite of the Elazig Magmatic Complex. This study investigates the geology, mineralogy, wall rock alteration, and geochemistry of the argentiferous ore and discusses formation conditions and sources of mineralizing fluids.

2. Geology

Two lithologic units are present in the study area (Fig. 2), (a) Coniacian–Campanian Elazig Magmatic Complex and, (b) its sedimentary cover the Eocene Kírkgeçit Formation.

The Elazig Magmatic Complex crops out over large areas in the Elazig and neighboring Malatya and Tunceli provinces. It consists of plutonic (gabbro, diorite,

* Corresponding author.
E-mail address: sagirogluahmet@hotmail.com (A. Sagiroglu).

1367-9120/03/$ - see front matter © 2003 Elsevier Ltd. All rights reserved.
doi:10.1016/S1367-9120(03)00101-9

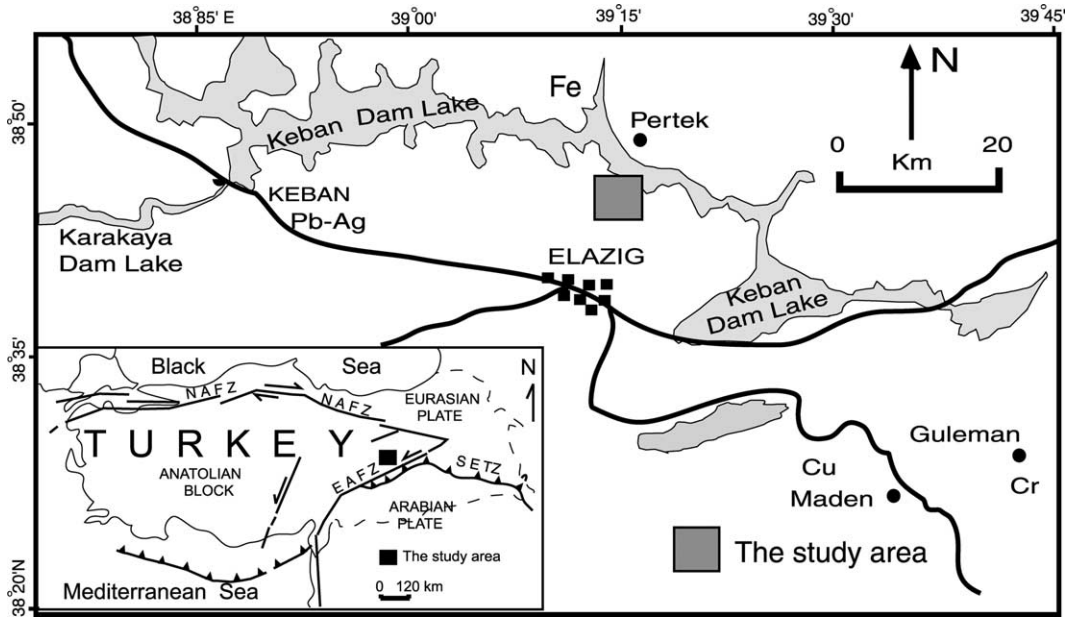

Fig. 1. Location of the studied area (NAFZ: North Anatolian Fault Zone; EAFZ: East Anatolian Fault Zone; SATZ: Southeast Anatolian Thrust Zone).

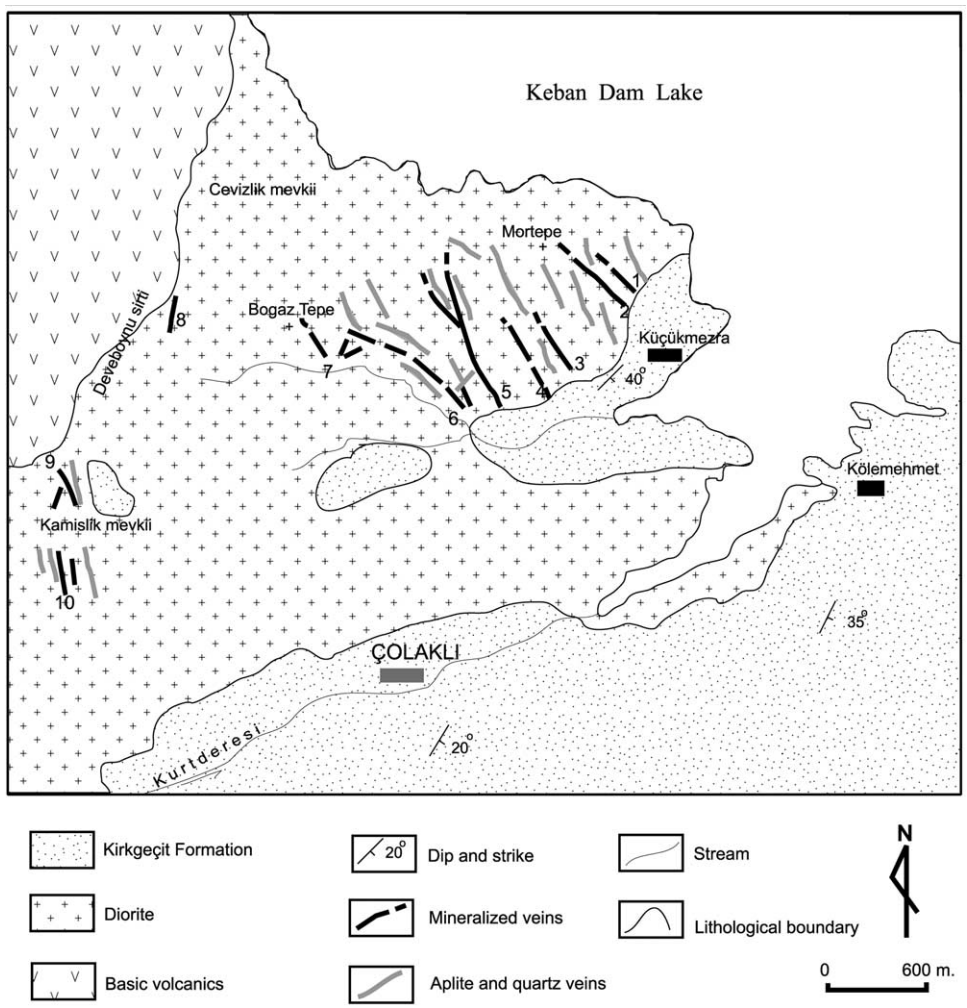

Fig. 2. Geological map of the studied area.

granodiorite, tonalite and granite), volcanic, subvolcanic (basalt, andesite, dacite and rhyolite), and pyroclastic lithologies (Yazgan, 1984). K/Ar absolute age determinations carried out by Yazgan (1984) yielded ages of 82–86 Ma for plutonic rocks and 74–80 Ma for volcanic rocks (i.e. Coniacian to Campanian).

Studies by Yazgan (1984), Asutay (1985), Bingöl (1984) and Akgül (1993) on the Elazig Magmatic Complex indicate that it is the product of arc magmatism, which was caused by north to south subduction. In fact, in chemical classification diagrams (Rb/SiO2, Nb/Y and Rb/Y + Nb), for rocks of the complex plot in the region of volcanic arc granite (VAG).

The epigenetic ore veins, which are the subject of this study, are emplaced in quartz diorite which is composed of plagioclase, hornblende, coarse-grained (~1 cm) biotite, quartz and K- feldspar. The basic volcanic rocks occupy large areas west and northwest of the mineralized area.

The Eocene sedimentary sequence consists of conglomerate and sandstone at the base, and sandy limestone, limestone and marl upwards (Avsar, 1983). The fractures and faults that bear veins and other formations are covered by the Kírkgeçit Formation, and therefore the veins are clearly pre- Eocene in age.

In the study area and vicinity, faults and fractures played a major role in ore formation since the Upper Cretaceous Eastern Taurus region and studied area have been deformed, by N–S compression. The main events that caused the deformations are; closure of the Tethys Ocean by northward subduction during the Late Cretaceous (Yazgan and Chessex, 1991; Sengör and Yílmaz, 1983), arc-continent collision during the Late Campanian (Yazgan and Chessex, 1991; Yazgan, 1984) and relative movements of the Arabian and Anatolian Plate since the collision. The deformations can be seen in all of the lithologies of the Elazig Magmatic Complex as fault and fracture systems. Most of the fault and fracture zones are filled with aplites, quartz–carbonate, microgranite and ores (Sagiroglu, 1986; Sasmaz, 1988).

The study area is densely faulted and major faults strike N35° to 50° W and dip vertically. The mineralized fault zones are readily distinguishable by their argillic wall rock alteration. The fault zones that are filled with mineralizations, aplites, microgranites and barren quartz run roughly parallel to each other and are apparently in the same fault system.

3. Ore formations

The Elazig Magmatic Complex gave rise to ore formations of various types and content. The best known of these are skarn -type argentiferous Pb–Zn deposits in Keban. Other ores that have similar mineralogical and geochemical compositions to those of Keban Pb–Zn ores, have been described by Sagiroglu (1986), Sagiroglu and Preston (1987) and Sasmaz and Sagiroglu (1990, 1999).

As described above; the Çolaklí ore bodies occur as veins in the fault zones (Fig. 2). Not all of the fault zones are mineralised. Some are filled by aplites, microgranite and barren quartz. Ten major mineralized zones were discovered. However, there may be more mineralized zones which are covered by thick soil overburden. The thickness of mineralized bodies (veins) varies between 0.5 and 2.5 m, and lengths range between 30 and 750 m.

The mineralized zones are accompanied by narrow but intense envelopes of wall rock alteration. Argillic (dominantly kaolinitic) alteration is the most common and silicification, carbonatization and vermiculite formation are also present.

The ore minerals are generally disseminated among barite, carbonate minerals and quartz in the veins. In places the ore becomes massive. The dominant ore minerals are either galena and freibergite, or chalcopyrite and the veins may be grouped in two types based on their dominant metal contents: (1) Pb–Ag veins and (2) Cu veins. Macroscopic features of the veins are summarized in Table 1.

Table 1
Geological features of studied mineralized veins

Vein no	Strike	Ore minerals	Gangue minerals	Thickness (cm)	Length (m)
1	N50°W	Galena	Calcite	20–25	80–100
2	N50°W	Galena, sphalerite, chalcopyrite	Quartz, calcite, siderite	40–50	250–300
3	N35°W	Galena, sphalerite	Calcite, rodokrozite	15–20	200–250
4	N30°W	Galena	Quartz, barite	50–200	250–300
5	N28°W	Galena, sphalerite, freibergite, tetrahedrite	Calcite, barite, kaolenite	50–350	750–800
6	N65°W	Galena, sphalerite, chalcopyrite, freibergite, tetrahedrite, cubanite	Calcite, siderite, rodokrozit kaolenite, barite, quartz	50–100	650–700
7	N35°W	Chalcopyrite, pyrite, galena	Calcite, barite	25–100	100–120
8	N15°W	Galena, sphalerite	Calcite, siderite	25–30	15–20
9	N25°W	Galena, chalcopyrite, sphalerite	Kaolenite	15–20	25–30
10	N10°W	Galena, sphalerite, chalcopyrite	Kaolenite, calcite, quartz	80–100	150–200

4. Ore microscopy

4.1. Ag–Pb veins

The Pb–Ag veins are the most common among the studied veins and are characterized by abundant galena and dense freibergite inclusions. Other common minerals are barite, sphalerite, chalcopyrite, fahlore (tetrahedrite-tennantite), pyrite, cubanite and a Pb–Cl phase.

Galena. This is the most abundant ore mineral in the Çolaklí veins and occurs as either massive fine-grained lumps or euhedral grains disseminated in mainly carbonate gangue matrix. Galena almost always contains inclusions of sphalerite, freibergite and tetrahedrite. These inclusions occur either

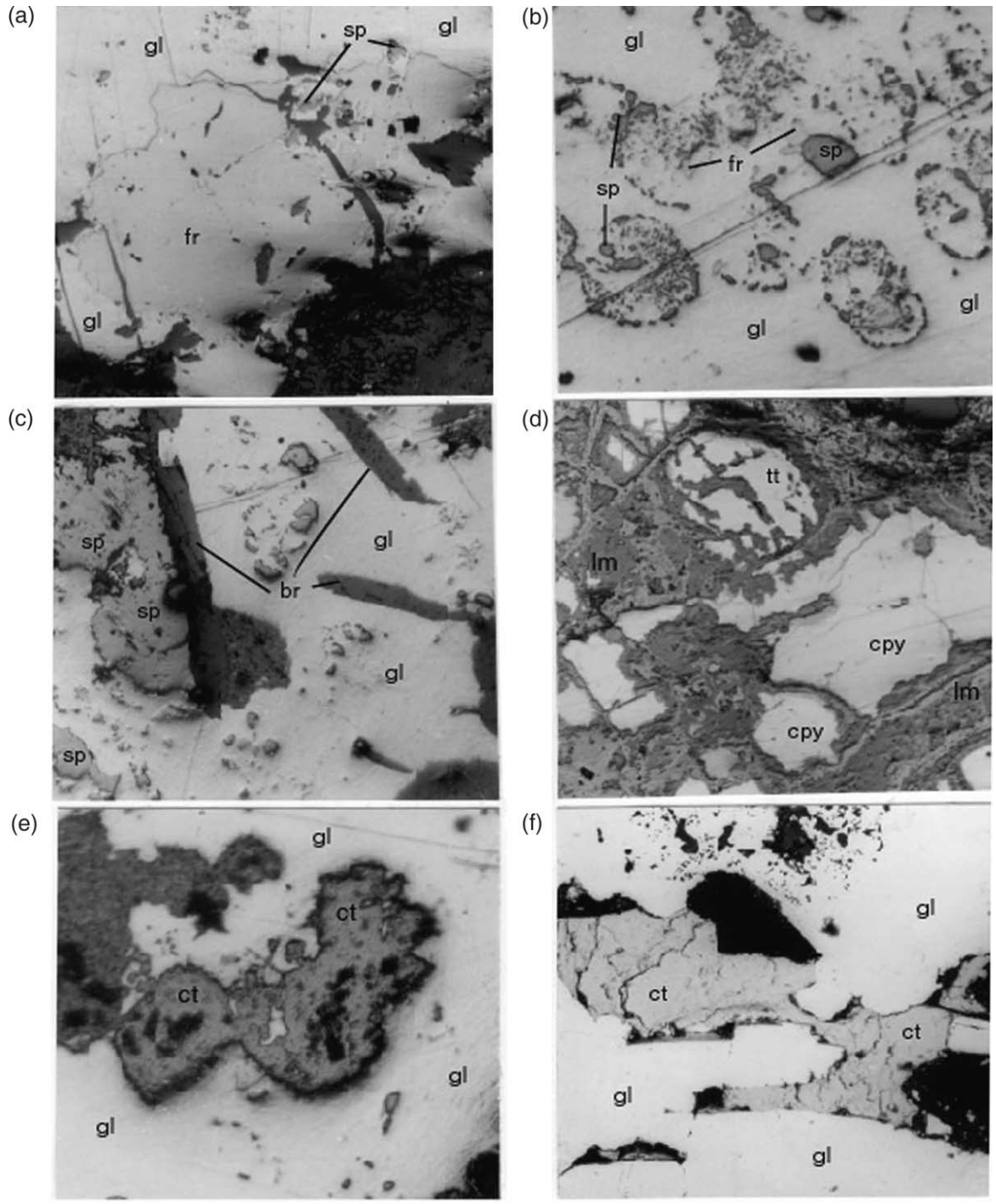

Fig. 3. (a). Randomly distributed sphalerite (sp) and freibergite (fr) inclusions in galena (gl). (b) Concentric or elliptic oriented sphalerite (sp) and freibergite (fr) inclusions in galena (gl). (c) Prismatic barite (br) crystals in galena (gl). (d) Chalcopyrite (cpy), tetrahedrite (tt) and limonite (lm). (e) Reflected light microscopic appearance of Pb–Cl phase (ct). (f). Back scattered electron image of Pb–Cl phase (ct).

Table 2
Geochemical analysis data of the studied samples (sample whose numbers start with leter R: wall rock samples; P: Pb–Zn vein samples; C: Cu vein samples)

Smp. no.	R25	R26	R27	R28	R36	R45	P21	P29	P30	P31	P32	P33	P37
Au (ppb)	18	<5	<5	<5	<5	<5	13	<5	<5	<5	<5	223	12
Ag (ppm)	<5	<5	<5	<5	<5	<5	12	440	1000	<5	<5	260	17
As (ppm)	15	6	4	31	10	4	9	36	100	21	2	28	8
Sb (ppm)	20	20	10	10	30	10	50	1960	4840	40	10	1330	30
Cu (ppm)	10	10	10	10	10	10	110	1810	4910	10	10	560	190
Pb (%)	<0.01	<0.01	<0.01	<0.01	0.04	<0.01	2.03	61.2	84.8	1.36	0.12	23.85	6.52
Zn (ppm)	20	30	30	460	591	30	990	20,100	14,300	726	25	16,200	2460
Ba (ppm)	360	470	700	1900	910	360	<100	60	3600	250	350	390	100
Cd (ppm)	<10	10	10	10	<10	<10	10	40	160	10	<10	50	10
Bi %	<0.01	<0.01	<0.01	<0.01	<0.01	<0.01	<0.01	<0.01	<0.01	<0.01	0.01	<0.01	<0.01
Ca (%)	2	<1	<1	<1	<1	<1	28	<1	<1	<1	2	3	29
Fe (%)	13	0.8	0.6	14.2	1.3	0.2	1.1	0.3	0.4	0.7	0.4	0.5	1.1
Na (%)	1.59	1.81	1.22	0.05	0.05	0.12	0.05	1.39	2.12	0.22	3.14	0.89	0.05
Mn (%)	0.01	0.01	0.01	4.2	1.44	0.01	1.42	0.01	0.07	0.18	0.01	0.06	0.89
La (ppm)	82	28	6	23	7	1	25	<1	<1	<1	5	36	35
Ce (ppm)	93	39	8	29	<3	3	40	<3	<3	<3	9	100	50
Nd (ppm)	17	9	<5	7	<5	<5	23	<5	<5	<5	<5	55	19
Sm (ppm)	2.1	1.4	0.4	2	0.2	<5	3.6	<0.1	<0.1	<0.1	0.4	13	3.6
Eu (ppm)	0.5	0.4	0.2	1.1	<1	<0.2	1.5	<0.2	<0.2	<0.2	0.2	2.2	1.7
Tb (ppm)	0.5	<0.5	<0.5	<0.5	<0.5	<0.5	1	<0.5	<0.5	<0.5	<0.5	2.8	0.6
Yb (ppm)	1.4	1.5	0.6	1.2	<0.2	<0.2	5.3	<0.2	<0.2	<0.2	<0.2	9.3	3.3
Lu (ppm)	0.19	0.24	0.1	0.2	<0.05	<0.05	0.86	<0.05	<0.05	<0.05	<0.05	0.17	0.52

Smp. no.	P39	P41	P43	P44	P46	P50	P51	P52	P53	C38	C42	C54
Au (ppb)	22	<5	<5	<5	<5	25	<5	<5	11	256	98	6
Ag (ppm)	37	<5	<5	<5	13	28	17	6	22	670	70	15
As (ppm)	44	43	14	24	10	19	11	4	9	1800	870	110
Sb (ppm)	290	30	20	20	50	330	60	20	30	8190	2610	180
Cu (ppm)	710	40	10	70	50	410	90	30	1410	29,620	24,640	19,320
Pb (%)	7.44	0.13	0.01	0.02	2.48	4.33	5.08	1.14	4.99	2.68	0.47	1.47
Zn (ppm)	1650	691	40	45	754	23,200	1290	810	2010	2870	1090	2430
Ba (ppm)	110	790	250	<100	1700	2300	3000	360	150	3100	<100	210
Cd (ppm)	20	10	<10	<10	10	200	10	10	30	290	10	40
Bi %	<0.01	<0.01	<0.01	<0.01	<0.01	<0.01	<0.01	<0.01	<0.01	0.04	0.32	<0.01
Ca (%)	21	5	<1	<1	23	17	26	32	29	23	<1	34
Fe (%)	0.9	7.1	0.9	1	2.3	1.1	2.4	1.1	1.9	1.4	7.3	4.1
Na (%)	0.05	0.05	0.65	2.58	0.86	0.05	0.05	0.05	0.05	6.1	0.05	0.05
Mn (%)	0.76	1.6	0.01	0.01	0.87	0.54	0.99	2.3	1.71	0.6	0.4	2.05
La (ppm)	28	27	13	41	27	93	32	16	17	36	6	17
Ce (ppm)	<3	28	9	48	33	120	42	36	36	44	9	39
Nd (ppm)	<5	8	<5	5	10	40	21	21	16	11	<5	25
Sm (ppm)	2.5	1.5	0.6	0.5	2.3	6.7	2.6	5.5	4.5	2.4	0.6	5.4
Eu (ppm)	<0.2	0.8	<0.2	<0.2	0.9	2.9	1.2	2.9	2.4	1.1	0.5	3
Tb (ppm)	<0.5	<0.5	<0.5	<0.5	<0.5	1.2	0.9	1.7	1	0.6	<0.5	<0.5
Yb (ppm)	<0.2	2.1	<0.2	1.1	2.1	3.6	3.4	6.1	3.5	2.4	<0.2	3.7
Lu (ppm)	<0.05	0.24	<0.05	0.14	0.36	0.58	0.57	0.81	0.57	0.45	<0.05	0.58

randomly distributed in galena, or in a very peculiar mode: minute (100–150 μm) euhedral grains of sphalerite, freibergite and tetrahedrite occur generally in circular or elliptic, and rarely as linear, orientations (Fig. 3(a) and (b)). Randomly distributed inclusions are found disseminated in galena grains, and have larger grain sizes (up to 500 μm). These type inclusions are apparently exsolutions or intergrowths with galena. In the second type, elliptic and linear orientations, the minute crystals of sphalerite and freibergite probably were concentrated in certain places of the Pb-phase and are intergrowths with galena.

Freibergite. Occurs almost always in galena and has a light whitish gray color and hardness close to galena. It is a very common mineral in Pb–Ag veins (Fig. 3(a) and (b)) as indicated by the high Ag content in the veins of up to 1000 ppm (Table 2). The freibergite grains disseminated in galena are larger in grain size and generally are not accompanied by sphalerite. Homogenous distributions in galena and lack of any orientation to the crystal growth planes indicate that these freibergites are exsolutions. In massive galena, freibergite occurs as described above. Rarely, freibergite is found also as individual grains.

Although precise microanalyses were not made, SEM analyses indicate that as Zn content of freibergite decreases, the color becomes lighter and whiter. A typical SEM EDS analysis of freibergite is given in Fig. 4.

Barite. Barite occurs as platy and prismatic crystals a few mm in size (Fig. 3(c)). In places it is the most abundant mineral.

Sphalerite. Sphalerite occurs throughout the ore formations (Fig. 3(b) and (c)). It is always a subsidiary mineral. Sphalerite occurs in two ways; as individual small grains or as inclusions coexisting with freibergite inclusions in galena. SEM EDS microanalysis and the transparent nature of sphalerite indicate a low Fe content that may indicate a low temperature of formation.

Fahlore (tetrahedrite- tennantite). Apart from freibergite, Cu–Zn fahlore is also present. Its color varies between light olive green to brownish gray and is distributed randomly.

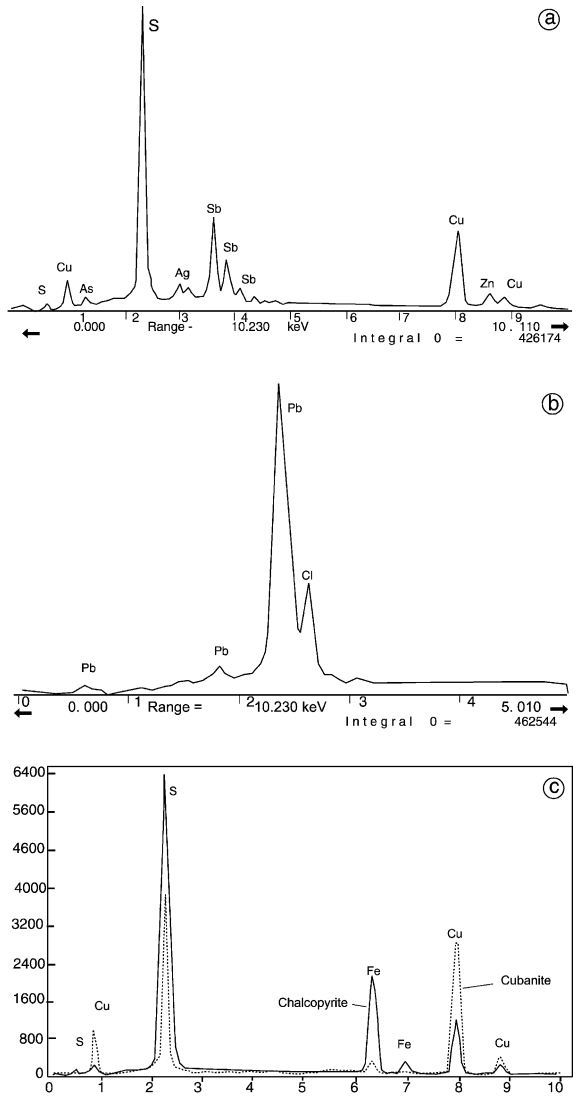

Fig. 4. SEM graphs of freibergite (a), Pb–Cl phase (b), cubanite and chalcopyrite (c).

Pb–Cl phase. Within massive galena ore, a Pb–Cl phase has been distinguished. Under reflected light it has a gray to bluish-gray color, earthy appearance and very low reflectance ($r = 15$) (Fig. 3(e)). SEM secondary electron image (Fig. 3(f)) shows lava-flow-like structures. SEM analyses (Fig. 4) indicate almost pure lead chlorid. Pure $PbCl_2$, cotunnite, has been known since 1825 and has been thoroughly investigated by modern workers because of its characteristic crystal structure (Leger et al., 1996; Haines et al., 1995, 1996). However, mineralogical features of the studied Pb–Cl phase do not resemble cotunnite that is white to yellowish and soft. Detailed microanalysis and XRD studies are needed to reveal the mineralogical aspects of this Pb–Cl phase. These studies are planned to be the subject of individual research.

Chalcopyrite. Chalcopyrite is found as small grains and does not contain any inclusions.

*Pyrite and cubanite*are present in minor amounts and occur as subhedral small grains.

4.2. Cu veins

In a few mineralized veins, Cu minerals (generally chalcopyrite and rarely cubanite) are dominant. These veins are readily distinguished in the field by their dark brown oxidation zones (gossans). Mineral paragenesis of these veins is chalcopyrite, pyrite, galena, sphalerite, cubanite, bismuthinite and fahlore.

Chalcopyrite. Occurs as large (up to 5 mm in grain size) crystals disseminated in gangue carbonate and quartz or forms massive lumps. It does not have any inclusions and displays various oxidation products, (covellite–chalcocite, cuprite, and limonite) in the weathered parts.

Pyrite. Pyrite is the second dominant mineral of the Cu veins and occurs as euhedral and un-zoned crystals mostly disseminated among other minerals.

Galena. Occurs as single grains and does not contain any kind of inclusions.

Sphalerite. Sphalerite grains are found always close to chalcopyrite crystals and some grains display chalcopyrite exsolutions.

Cubanite. It has a lighter color than chalcopyrite and strong anisotropy. Although the common form of cubanite is lamellar or ‘sharply bounded laths’ in chalcopyrite (Ramdohr, 1980; Craig and Vaughan, 1981), it occurs in studied samples as separate grains without any lamellar features. SEM studies show that cubanite does not have any inclusions or zoning. The composition of a cubanite in relation to that of chalcopyrite is given in Fig. 4.

Bismuthinite. Its color reflectance and hardness are quite similar to those of galena but differs from it by its rarity, color and strong anisotropy.

Fahlore. Small amounts of freibergite and common tetrahedrite–tennantite are present in Cu veins (Fig. 3(d). They have similar aspects to Pb–Ag veins.

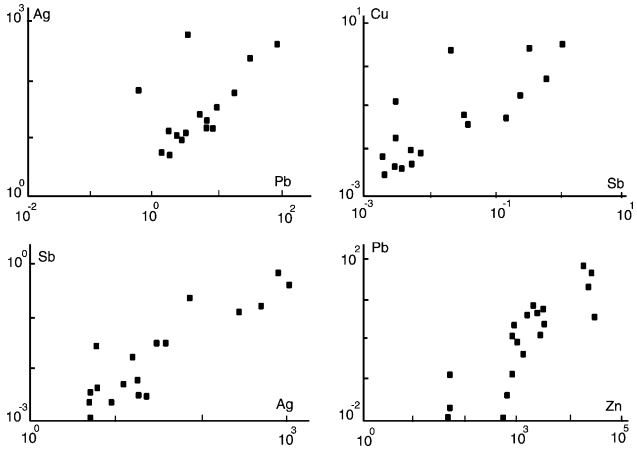

Fig. 5. Correlation relationships for some major and minor elements of the veins.

5. Geochemistry

Polished and thin sections of randomly collected samples from the veins were studied with SEM following microscopic studies. In addition, the samples were analyzed for major and minor elements and REE using ICP and neutron activation methods.

5.1. Major and minor elements

Major and minor element geochemistry of vein samples are given in Table 2. As can be seen in the table, Pb, Cu and Zn contents reach up to 84.8, 2.46 and 2.32%, respectively. High As, Sb and Ag contents should originate from fahlores: freibergite and tetrahedrite–tennantite. This is proven by high correlation values between Sb–Ag, Sb–Cu and Sb–As pairs (Fig. 5). Apparently most of the Cu occurs in fahlore minerals as indicated by correlation between Cu–As and Cu–Sb.

Similarly, high Pb–Zn and Pb–Ag correlation values reflect the microscopic evidence of close association between galena and sphalerite, and the existence of Ag bearing phases only within galena grains. Very low correlation values of Ba–Pb and Ba–Zn indicate that barite and galena–sphalerite associations are not intergrowths. Instead, they were enriched in different places and probably in different phases. Although no Cd mineral has been detected by microscopic and SEM studies, the Cd content in ore samples can be as high as 2900 ppm (Table 2). It is well known that sphalerite structure accommodates high amounts of Cd as a result of ionic exchange between Cd–Zn. However, low correlation value ($r = 0.52$) between Cd–Zn only partly meets this expectation. High correlation values between Cd–Sb, Ag–Cd and Cd–Ba pairs (0.81, 0.66, 0.68, respectively), do not have reasonable explanations; any Cd phase coexisting with freibergite and other fahlores was not determined. Ionic exchanges between Cd–Sb and Cd–Ba are not possible since Cd^{+2} has an ionic radius 0.97 Å while the ionic radii of Sb^{+3} and Ba^{+2} are 0.88 and 1.35 Å, respectively. Ionic exchange is only possible between Cd^{+2} and Ag^{+2} that have ionic radii of 0.97 and 0.89 Å, respectively. Although Bi minerals are very rare in the mineralized parts, Bi contents reach up to 3200 ppm in the studied samples that have small bismuthinite crystals. Bi does not correlate significantly with the other cations present.

5.2. Rare earth elements

The studied vein samples and host rocks were analyzed for Y, La, Ce, Nd, Sm, Eu, Tb, Yb and Lu. As can be seen from the analytical data, most of the values are higher than those of the quartz diorite host rock and averages given for intermediate rocks by Wedepohl (1978) (Table 3).

Normalized REE patterns of mineralized veins and magmatic rocks are shown in Fig. 6. The REE patterns of quartz diorite, Cu veins, and granite have similar trends, suggesting a close relationship. Pb veins usually have higher values than host magmatic rocks according to studies of Taylor and Fryer (1983), Oreskes and Eunaudi (1990) and Fleet et al. (1997) on various mineralizations. Higher REE contents in the mineralized parts are common because of the incompatible nature of REE. Furthermore, in previous

Table 3
REE contents of veins and various rocks (as ppm)

REE	Average of intermediate rocks (Wedepohl, 1978)	Average of quartz diorite (Wedepohl, 1978)	Vein samples		BK-2	K-20	BK-5	BK-1	BK-3
			Highest	Average					
Y	35	10.6	–	–	10	<10	<10	<10	<10
La	31	15.5	93	35	39	5	15	36	38
Ce	60	20.7	120	48	54	6	21	38	43
Nd	31	8.1	55	18	13	<5	7	8	12
Sm	6.2	2.8	6.7	3.7	2.5	0.2	1.6	1.3	1.5
Eu	1.3	0.38	2.9	1.4	0.7	<0.2	0.7	0.3	<0.2
Tb	1.1	0.36	2.8	0.7	<0.5	<0.5	0.8	<0.5	<0.5
Yb	3.8	0.16	9.3	3.1	1.5	0.4	1	1.8	2
Lu	0.62	0.07	0.86	0.41	0.26	0.09	0.14	0.37	0.39

BK-2: Quartz diorite, K-20: Aplite, BK-5: Microgranite, BK-1 and BK-3: Granite.

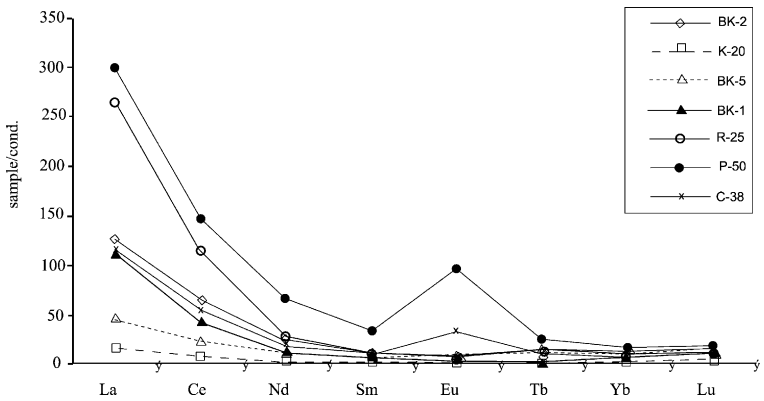

Fig. 6. Normalized REE patterns of studied veins and host plutonic rocks (BK-2: Quartz diorite; K-20: Aplite; BK-5: Microgranite; BK-1: Granite; R25: Barren; Pb-V1: Sample P50; Cu-V1: Sample C38).

studies (Thode et al., 1991; Oreskes and Eunaudi, 1990) LREE increases are significant and HREE increases are also present. In the studied veins, REE patterns exhibit similar trends (see Fig. 6). According to Palacios et al. (1986) REE contents may indicate the stage of Cu–Ag mineralization; first stage having a low REE increase and the last stage a high increase. High REE increases in the studied Pb veins can be interpreted as occurring after magmatism as indicated by field and microscopic data. Some previous studies evaluated REE contents in estimating physico-chemical conditions of ore forming hydrothermal solutions. According to Bau (1991). , a La/Lu ratio >1 and positive Eu anomaly indicate mildly acidic conditions. The studied samples always meet these conditions and mineral paragenesis (sulphides and sulphosalts) indicates an acidic condition. Lottermoser (1989) claims that high As and Eu values indicate reducing high temperature conditions. In the Çolaklí samples, As rich samples are Eu poor (Table 2). This and all the previously mentioned data show a reducing but low temperature of formation.

The studied samples do not show any significant correlation (positive or negative) between REE and metallic elements. Significant correlation values are either among the metallic elements themselves or between REE.

In general, normalized REE patterns of mineralized veins, quartz diorite and granitic rocks of the Çolaklí area are similar and may indicate a single origin for all three a magmatic source for the mineralizing hydrothermal solutions.

6. Conclusions

Mineralized veins are clearly epigenetic and fill part of the N10°–60° W striking and almost vertical fault/fracture system. The same fracture system contains microgranite and barren aplite and quartz (± carbonates) dikes that run parallel to the ore veins. Apparently all were products of the last phases of magmatism and filled the fracture system in diorite.

Wall rock alteration occurs as narrowly developed zones around mineralized veins and is composed of clay minerals and vermiculite, in addition to exhibiting silicification and carbonitization.

Two types of veins are distinguished according to their dominant metallic element; Pb–Ag veins and Cu veins. The ore minerals of the Pb–Ag veins are galena, freibergite, fahlore, sphalerite, baryte, chalcopyrite, cubanite, baryte, pyrite and a Pb–Cl phase. Freibergite occurs generally as minute crystals forming elliptic or circular concentrations in galena together with minute sphalerite and tetrahedrite crystals. This may be interpreted as the presence of unmixing phases prior to crystallization. Probably, during galena crystallization, pockets bearing As, Ag and Zn phases formed and these phases crystallized a little later than galena. Cu veins contain ore minerals of higher formation temperatures such as cubanite, chalcopyrite, bismuthinite, tetrahedrite and sphalerite. Therefore, it is reasonable to conclude that Cu veins formed earlier than Pb–Ag veins. This claim is supported by evidence indicating low temperature formation for the Pb–Ag veins. The evidence can be summarized as follows;

1. Kaolinite dominant wall rock alteration,
2. Presence of high amounts of barite,
3. High Ag content,
4. Pockets of small crystals in galena.
5. Very high LREE and high HREE contents.

REE patterns indicate a very close association between Cu and quartz diorite and Pb–Ag veins.

The close association of veins with late phase magmatic products such as quartz veins, aplites and microgranites, the parallel trends of REE patterns for wall rock, aplites and ore, and emplacement of the mineralized veins in magmatic rocks all suggest that the hydrothermal solutions responsible for ore formation evolved from a magmatic source.

As stated before, many Ag-rich Pb–Zn ores are associated with the Elazig Magmatic Complex. The Keban Pb–Zn deposits are the most important and numerous small veins are present in the neighboring areas

of Çolaklí. Their mineralogy, especially Ag-bearing minerals, show little variation. The mineral assemblages of the deposits and their relationship with the magmatic complex are as follows; Pyrometasomatic Keban Ore Deposits have the mineral assemblage pyrite, löllingite, galena, sphalerite, arsenopyrite, native Ag and Ag–tetrahedrites (Kines, 1971). Kízíldag Pb–Zn veins in granite have the mineral assemblage galena, sphalerite, pyrite, arsenopyrite, chalcopyrite and Ag–tetrahedrites (freibergite) (Sagiroglu and Preston, 1987). The similarities in ore mineralogy may point out that all these ore formations are part of a regional ore system and may therefore have considerable economic potential.

Acknowledgements

This research is carried out as a TUBITAK project (YDAB"ÇAG-379). We sincerely thank to TUBITAK. SEM studies were made in the Earth Science Department of Berlin Technical University. We thank the colleagues and technicians of the BTU. Prof. Dr C. Helvaci (Dokuz Eylül University) and Prof. Dr S. Kirikoglu (Istanbul Technical University) are thanked for reviewing the manuscript.

References

Akgül, B., 1993. Piran Köyü çevresindeki magmatik kaya"çlarín petrografik ve petrolojik özellikleri. F.Ü.Fen Bil. Ens., Doktora Tezi (unpublished), 128 s. Elazig.

Akgül, B., Sasmaz, A., 1996. Elazig kuzeyinde pirometazomatik olusuklar ve iliskili Fe–Ti cevherlesmeleri. Türkiye Jeoloji Bülteni, C 39/2, 39–49.

Asutay, H.J., 1985. Baskil (Elazig) çevresinin jeolojik ve petrografik incelenmesi. A.Ü.Fen Bil. Enst., Doktora Tezi (unpublished), 176 s., Ankara.

Avsar, N., 1983. Elazig yakín kuzeybatísında stratigrafik ve mikropaleontolojik arastírmalar. F.Ü. Bil. Ens. Doktora Tezi, (unpublished), 84 s, Elazig.

Bau, M., 1991. Rare-earth element mobility during hydrothermal and metamorphic fluid–rock interaction and the significance of the oxidation state of europium. Chem. Geol. 93, 219–230.

Bingöl, A.F., 1984. Geology of the Elazig area in the Eastern Taurus Region. Int. Sym.; Geol. Taurus Belt. Proc., Ankara, 209–216.

Craig, J.R., Vaughan, D.J., 1981. Ore Microscopy and Ore Petrography, Wiley, New York, 406 p.

Fleet, M.E., Seller, M.H., Pan, Y., 1997. REE, protoliths and alteration at the Hemlo Gold Deposits, Ontario, Canada and comparison with argillic and serisitic alteration in the Highland Valley Porphyry District, British Columbia, Canada. Econ. Geol. 92, 551–568.

Haines, J., Leger, J.M., Atouf, A., 1995. Crystal-structure and equation of cotunnite-type zirconia. J. Am. Ceram. Soc. 78 (Issue 2), 445–448.

Haines, J., Leger, J.M., Schulte, O., 1996. The high-pressure phase-transition sequence from the rutile-type through to the cotunnite-type structure in PbO2. J. Phys.-Condens. Matter 8/11, 1631–1646.

Kines, T., 1971. The geology and the ore mineralization in Keban area, PhD thesis (unpublished), Durham University, UK, 250 p.

Leger, J.M., Haines, J., Atouf, A., 1996. The high-pressure behavior of the cotunnite and post-cotunnite phases of $PbCl_2$ and $SnCl_2$. J. Phys. Chem. Solids 57/1, 7–16.

Lottermoser, B.G., 1989. REE behavior associated with strata-bound scheelite mineralization (Broken Hill, Australia). Chem. Geol. 78, 119–134.

Oreskes, N., Eunaudi, M.T., 1990. Origin of REE-enriched hematite breccias at the Olympic Dam Cu-U–Au–Ag Deposits, Roxby Downs, South Australia. Econ. Geol. 85, 1–28.

Palacios, C.M., Hein, U.F., Dulski, P., 1986. Behavior of REE during hydrothermal alteration at the Buena Esperanza copper–silver deposits, Northern Chile. Earth Planet. Sci. Lett. 80, 208–216.

Ramdohr, P., 1980. The ore minerals and their intergrowths, Academia-Verlag, 1202 p.

Sagiroglu, A., 1986. Kízíldag (Elazig) cevherlesmelerinin özellikleri ve kökeni. Jeoloji Müh.Odasí Bült 29, 5–13.

Sagiroglu, A., Preston, R.M.F., 1987. Ore mineralogy of Kízíldag Pb–Zn veins-with a special emphasis on the composition of the tetrahedrites. J. Fírat Univ. 2, 83–94.

Sagiroglu, A., 1992. Pertek-Demürek (Tunceli) skarn tipi manyetit ve iliskili bakír cevherlesmeleri. TJK Bülteni 35, 63–70.

Sasmaz, A., 1988. Billurik Dere (Elazig) cevherlesmelerinin özellikleri ve kökeni. F.Ü.Fen Bil. Enst. Yüksek Lisans Tezi, 63 s.

Sasmaz, A., Sagiroglu, A., 1990. The features and origin of Billurik Dere (Elazig) mineralizations. Bull. Miner. Res. Explor. 110, 45–54.Ankara.

Sasmaz, A., Sagiroglu, A., 1999. Çolaklí (Harput–Elazig) damar tipi Pb–Zn cevherlesmelerinin jeolojisi. Türkiye Jeoloji Bülteni 42/2, 17–24.Ankara.

Sengör, A.M.C., Yílmaz, Y., 1983. Tetheyan evolution of Turkey: a plate tectonic approach. Tectono Phys. 75, 181–241.

Taylor, R.P., Fryer, B.J., 1983. Rare earth element litho-geochemistry of granitoid mineral deposits. Canad. Ins. Min. Metallogeny Bull. 76, 74–84.

Thode, H.G., Ding, T., Crocket, J.H., 1991. Sulphur-isotope and elemental geochemistry studies of the Hemlo gold mineralization, Ontario: sources of sulphur and implications for the mineralization process. : Canad. J. Earth Sci. 28, 13–25.

Yazgan, E., 1984. Geodynamic evolution of the Eastern Taurus region. Int. Symp. Geol. Taurus Belt, Proc., Ankara, 199–208.

Yazgan, E., Chessex, R., 1991. Geology and tectonic evolution of the southeastern Taurides in the region of Malatya. TBAG Bull. V.3/1, 1–42.

Wedepohl, K.H., 1978. Handbook of Geochemistry, vol. 5. Springer, Berlin.